Korean J. Chem. Eng., 40(1), 91-96 (2023)
DOI: 10.1007/s11814-022-1282-1

pISSN: 0256-1115
eISSN: 1975-7220

Catalytic removal of VOCs using Pt loaded on used battery derived Zn

Young-Kwon Park*, Sang-Chul Jung, Ho-Young Jung***, and Sang Chai Kim****,†**

*School of Environmental Engineering, University of Seoul, Seoul 02504, Korea
**Department of Environmental Engineering, Sunchon National University, Sunchon 57975, Korea
***Department of Environment and Energy Engineering, Chonnam National University, Gwangju 61186, Korea
****Department of Environmental Education, Mokpo National University, Muan 58554, Korea
(*Received 13 July 2022 • Revised 22 August 2022 • Accepted 4 September 2022*)

Abstract−In order to investigate the feasibility of applying Zn rods (ZR) from spent primary batteries (SPBs) as a catalyst support for the complete oxidation of volatile organic compounds (VOCs), the prepared Pt catalyst based on Zn rod (Pt/SZR) was tested for the oxidation of benzene, toluene, and o-xylene. The catalyst's basic properties of Pt/SZR catalysts were characterized by BET analysis, XRD, H_2-TPR, SEM/EDX, TEM and XPS. The main ingredient of ZR was zinc oxide. As expected, for the Pt/SZR catalyst, increasing the amount of Pt added to the SZR from 0.1 wt% to 1.0 wt% increased the conversions of benzene, toluene, and o-xylene. The reaction temperature for complete oxidation of benzene, toluene, and o-xylene over the 1.0 wt% Pt/SZR catalyst was less than 310 °C at GHSV of 50,000 h^{-1}. TEM, XPS, and H_2-TPR analysis indicated that the increase in catalytic performance due to Pt added was attributed to the active component (Pt species) and also to the readily movable lattice oxygen. This results indicate that ZR of SPBs is promising as a catalyst support for the oxidation of VOCs.

Keywords: Used Battery, Zinc Rod, Platinum, Complete Oxidation, VOCs

INTRODUCTION

The annual consumption of batteries is estimated to be 8 billion units per year in the USA and Europe, 6 billion in Japan, and 1 billion in Brazil [1]. Also, China has produced more than 15 billion acidic or alkaline Zn/Mn batteries annually since 2002 [2]. The increasing use of electrical and electronic products that are traditionally powered by primary batteries will also increase the demand for primary batteries [3]. Accordingly, the amount of spent primary batteries generated will also increase. Because discarded batteries contain toxic substances, landfill can contaminate soil, water, crops, and fisheries, and ultimately be harmful to human health [4]. In addition, Wang et al. [5]'s report on ecotoxicological assessment of spent battery extract showed significant environmental issues. Therefore, spent primary batteries must be disposed of safely to protect the ecosystem. Much attention has been paid to the recycling of spent primary batteries. As part of that, many research efforts have been conducted to recover valuable metals from spent primary batteries [6,7].

Volatile organic compounds (VOCs) are known air pollutants. Three major categories of environmental carcinogens contain o-xylene, toluene, and benzene among VOCs. o-Xylene, toluene, and benzene represent serious health hazards, and to prevent air pollution, need to be removed. The various technologies to reduce VOCs include condensation [8], adsorption [9], membrane separation [10], photocatalytic decomposition [11], plasma oxidation [12], biological decomposition [13], combustion [14] and catalytic oxidation [15]. Catalytic oxidation with a catalyst is an excellent technology for reducing VOCs, because the production of nitrogen oxides is lower than that of thermal oxidation, the operating cost is relatively low, and the removal efficiency is high [16-18]. In general, transition metal-based catalysts or precious metal-based catalysts are frequently adapted as catalysts for VOCs oxidation [19-22]. Since spent primary batteries contain manganese and zinc, which are known catalysts for organic compounds oxidation, it is likely that spent primary batteries could be used to provide a catalyst material for VOCs oxidation. Hassan et al. recovered zinc oxide nanoparticles from spent Zn-C batteries, and prepared a ZnO sensor for VOC detection [23]. Gallegos et al. synthesized MnZnO catalyst from waste alkaline and Zn/C batteries for VOCs removal [24]. Zhao et al. [25,26] prepared spent Zn-Mn core powders, and used them to synthesize a photo-catalyst for toluene removal.

Wang et al. [27] prepared ZnO, MgO, and Al_2O_3 nanoparticles and loaded Au. They reported that the catalytic performance of Au/ZnO was much better than that of Au/MgO and Au/Al_2O_3 in the catalytic oxidation of benzene, toluene, and p-xylene. Inside the primary battery of D company, there was a black mass composed of carbon and manganese, and a zinc rod composed of zinc oxide. This work investigated if the zinc rod of spent batteries could be used as a catalyst support. We prepared a catalyst support (SZR) from zinc rods of spent primary batteries, and loaded Pt (Pt/SZR). The Pt/SZR catalyst was used to achieve the complete oxidation of VOCs, o-xylene, toluene, and benzene chosen as a model VOC.

EXPERIMENTAL DETAILS

1. Catalysts

The zinc rod (ZR) found in the center of spent primary batter-

†To whom correspondence should be addressed.
E-mail: gikim@mokpo.ac.kr

Fig. 1. A picture of the inside of a spent battery.

ies of R company was treated with 0.1 N sulfuric acid solution to prepare the SZR. Fig. 1 shows the zinc rod of the spent primary battery. Section S1 of the Supplementary Information (SI) describes the preparations of SZR and Pt/SZR catalysts, while Section S2 of the SI provides the instrumental analyses, namely BET, SEM/EDX, XRD, H_2-TPR, ICP/OES, and FE/TEM.

2. Catalytic Oxidation

An oxidation reaction experiment was conducted in a conventional fixed reactor, as described in earlier work [28]. In addition, Section S3 of the SI provides the detailed experimental procedures and the analytical methods.

Table 1. Elemental components of SZR catalysts measured by SEM/EDX

Element	C	O	Zn
SZR	6.2	20.7	73.1

RESULTS AND DISCUSSION

1. Catalyst Characterization

SEM/EDX measurements were carried out to investigate the surface chemical components of the SZR. Fig. 2 shows the SEM image and the corresponding EDX spectra for the SZR. Table 1 summarizes its elements according to the EDX spectra. The surface components of the SZR are composed of 6.2% carbon, 20.7% oxygen, and 73.1% zinc.

Fig. 3 shows the morphologies of the SZR, 0.1Pt/SZR, 0.3Pt/SZR, 0.5Pt/SZR, and 1.0Pt/SZR catalysts at 20,000 times magnification. The SEM image of the SZR shows that the columnar particles are distributed on the catalyst surface (Fig. 2(a)). However, the addition of platinum to the SZR led to a change in form from columnar to flat plate (Figs. 2(b)-(e)). Furthermore, as the amount of platinum increased, small particles were formed evenly on the catalyst surface.

Fig. 4 shows the crystalline phases of the catalysts determined by XRD. Although zinc and carbon were present in the EDX result of SZR, the XRD profile of SZR showed a diffraction peak for zinc oxide (ZnO) alone. Accordingly, carbon species did not appear to have developed crystallinity. The XRD results of the Pt/SZR catalysts did not show crystalline phase representing platinum species, suggesting that the low concentration of platinum species was very well distributed on the catalyst surface, and thus the crystalline phase of platinum species was poorly developed [29]. The addition of platinum to the SZR did not change its original crystalline phase.

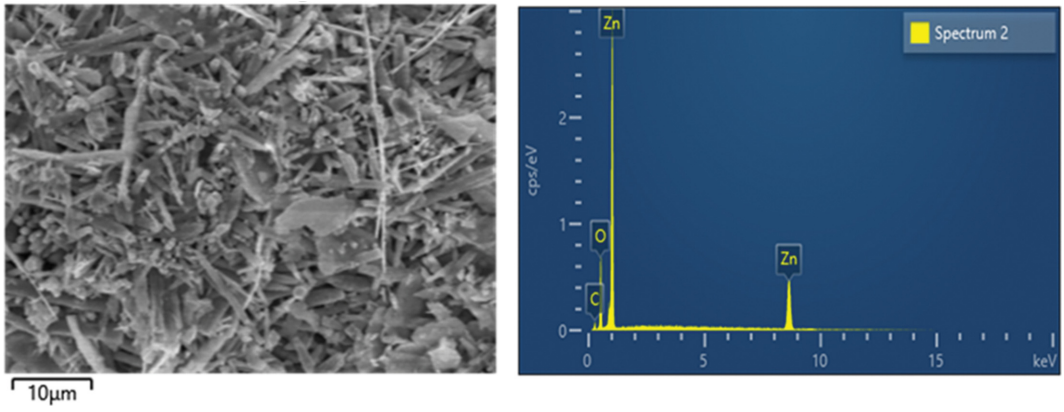

Fig. 2. SEM photomicrograph and corresponding EDX spectra for SZR.

Table 2. Binding energy values (eV) of the 0.1Pt/SZR, 0.3Pt/SZR, 0.5Pt/SZR, and 1.0Pt/SZR catalysts

Catalyst	0.1Pt/SZR		0.3Pt/SZR		0.5Pt/SZR		1.0Pt/SZR	
Orbit	Pt^{+2}	Pt^{+4}	Pt^{+2}	Pt^{+4}	Pt^{+2}	Pt^{+4}	Pt^{+2}	Pt^{+4}
4f7/2	72.18	-	72.29	74.41	72.32	74.45	72.21	74.61
4f5/2	75.06	-	75.10	77.87	75.01	77.91	75.12	78.09

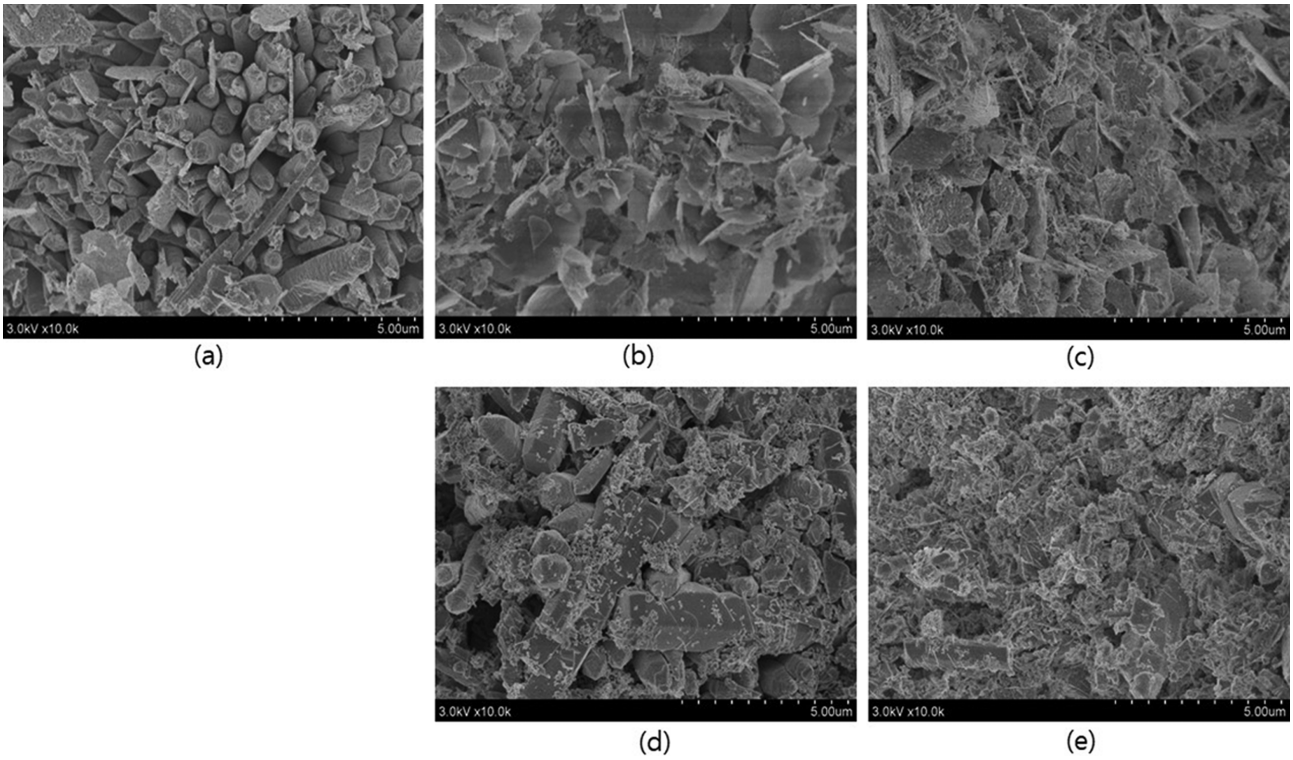

Fig. 3. SEM pictures of (a) SZR, (b) 0.1Pt/SZR, (c) 0.3Pt/SZR, (d) 0.5Pt/SZR, and (e) 1.0Pt/SZR catalysts.

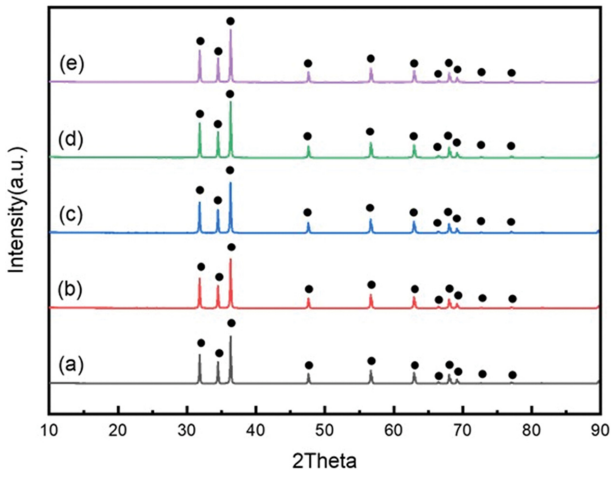

Fig. 4. XRD profiles (a) SZR, (b) 0.1Pt/SZR, (c) 0.3Pt/SZR, (d) 0.5Pt/SZR, and (e) 1.0Pt/SZR catalysts. ● ZnO.

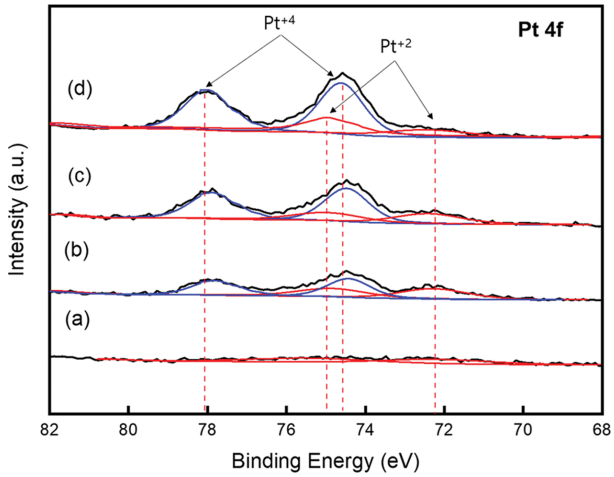

Fig. 5. XPS spectra (a) 0.1Pt/SZR, (b) 0.3Pt/SZR, (c) 0.5Pt/SZR, and (d) 1.0Pt/SZR catalysts.

The oxidation states of surface species on 0.1Pt/SZR, 0.3Pt/SZR, 0.5Pt/SZR, and 1.0Pt/SZR catalysts were characterized by XPS analysis.

Fig. 5 shows the XPS spectra of platinum of the catalysts, while Table 2 summarizes their binding energies (BEs). The binding energies (BEs) of platinum at $4f_{7/2}$ and $4f_{5/2}$ for 0.1 wt% Pt/SZR catalyst were (72.18 and 75.06) eV, respectively, which correspond to the platinum oxide state (Pt^{+2}) [30,31]. In addition, two platinum oxide states (Pt^{+2}, Pt^{+4}) were observed in the 0.3Pt/SZR, 0.5Pt/SZR,

Table 3. BET surface areas, mean pore diameters, and total pore volumes of SZR, 0.1Pt/SZR, 0.3Pt/SZR, 0.5Pt/SZR, and 1.0Pt/SZR catalysts

Catalyst	SZR	0.1Pt/SZR	0.3Pt/SZR	0.5Pt/SZR	1.0Pt/SZR
BET surface area (m^2/g)	3.16	5.09	5.18	5.39	5.82
Mean pore diameter (nm)	51.68	42.87	41.45	39.32	40.31
Total pore volume ($cm^3\ g^{-1}$)	0.04	0.05	0.05	0.05	0.05

Table 4. Temperature of TPR peaks of SZR, 0.1Pt/SZR, 0.3Pt/SZR, 0.5Pt/SZR, and 1.0Pt/SZR catalysts

Catalyst	SZR	0.1Pt/SZR	0.3Pt/SZR	0.5Pt/SZR	1.0Pt/SZR
Temperature of TPR peak (°C)	514	503	461	453	452

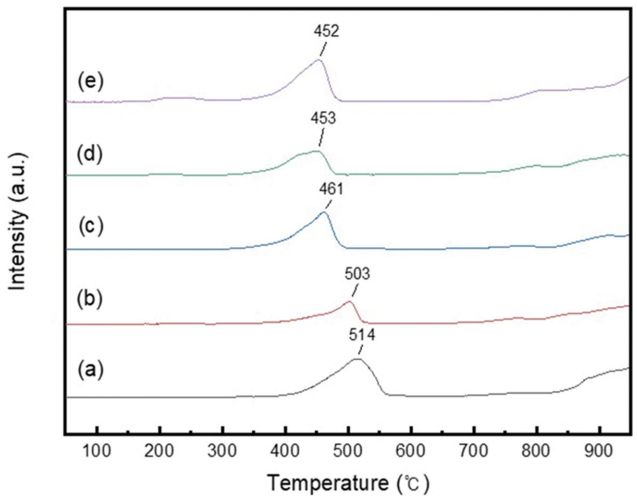

Fig. 6. TPR patterns of (a) SZR, (b) 0.1Pt/SZR, (c) 0.3Pt/SZR, (d) 0.5Pt/SZR, and (e) 1.0Pt/SZR catalysts.

& 1.0Pt/SZR catalysts. The BEs of $4f_{7/2}$ and $4f_{5/2}$ for 0.3Pt/SZR catalyst were (72.29 and 74.41, 75.10 and 77.87) eV, respectively. The BEs of platinum of the 0.3Pt/SZR catalyst fall into the characteristic category of the platinum oxide state (Pt^{+2}, Pt^{+4}) [30,31]. The 0.5Pt/SZR and 1.0Pt/SZR catalysts also showed BEs values having two oxidation states (Pt^{+2}, Pt^{+4}). As the amount of platinum added to the SZR increased, the intensity of the XPS peak also increased.

The textural properties of the catalysts were investigated by BET measurement. Table 3 lists the BET surface areas, mean pore diameters, and total pore volumes of the five catalysts. When platinum was added to the SZR from (0.1 to 1.0) wt%, as the amount of platinum added to the SZR increased, the BET surface area increased. The increase in BET surface area seemed to be related to the increasingly uniform dispersion of small particles on the catalyst surface as the amount of platinum added to the SZR increases, as shown in Fig. 3. Mean pore diameter decreased up to the platinum addition amount of 0.1 wt%, and was constant within the range of experimental error at the addition amount of 0.3 wt% or more. The total

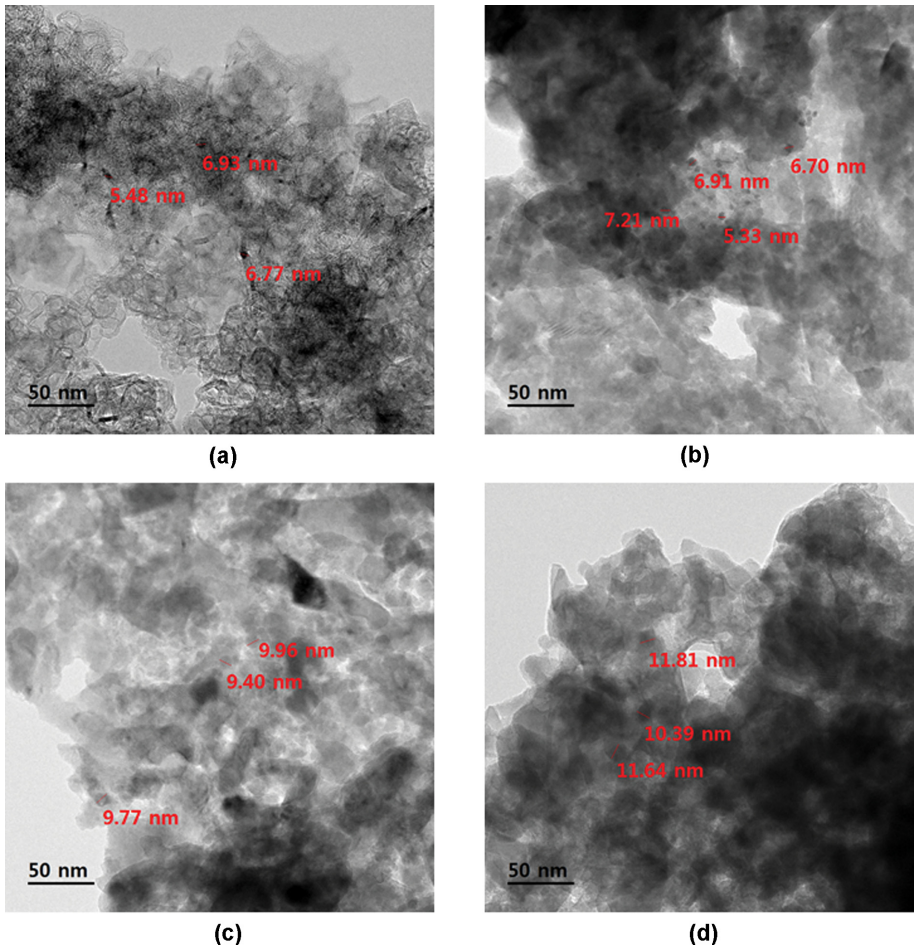

Fig. 7. FE/TEM pictures of (a) 0.1Pt/SZR, (b) 0.3Pt/SZR, (c) 0.5Pt/SZR, and (d) 1.0Pt/SZR catalysts.

pore volume of the SZR was 0.04 cm^3g^{-1}, while those of the (0.1-1.0) wt% Pt/SZR catalysts were identical at 0.05 cm^3g^{-1}.

Fig. 6 and Table 4 show the TPR profiles and temperature of TPR peak for all samples. A major reduction peak was observed in the TPR profile of the SZR. TPR profiles of the 0.1Pt/SZR, 0.3Pt/SZR, 0.5Pt/SZR, and 1.0Pt/SZR catalysts were similar to that of the SZR, consisting of one reduction peak that started at around 345 °C. Accordingly, this peak was attributed to the reduction of zinc oxide. Lowering the reduction temperature of catalyst lattice oxygen makes the movement of lattice oxygen easier, increasing the catalytic activity of hydrocarbon oxidation [32,33]. As shown in Fig. 4, the addition of platinum to the SZR lowered the reduction temperature of lattice oxygen of the SZR, and as the amount of platinum added increased, the lattice oxygen mobility of the Pt/SZR catalyst increased.

Fig. 7 shows the FE/TEM images of the 0.1Pt/SZR, 0.3Pt/SZR, 0.5Pt/SZR, and 1.0Pt/SZR catalysts. The particle sizes of platinum for the 0.1Pt/SZR, 0.3Pt/SZR, 0.5Pt/SZR, and 1.0Pt/SZR catalysts were in the range ((5.48-6.93), (5.33-7.21), (9.40-9.96), & (10.39-11.81)) nm, respectively. As the amount of platinum added to the SZR increased, the particle size of platinum increased.

2. BTX Oxidation

The o-xylene, toluene, and benzene conversions were measured for the performance of each catalyst according to reaction temperatures over the SZR, 0.1Pt/SZR, 0.3Pt/SZR, 0.5Pt/SZR, and 1.0Pt/SZR catalysts.

Figs. 8(a), (b), and (c) show the conversion curves of o-xylene, toluene, and benzene, respectively. As expected, experimental results indicate the amount of platinum added to the SZR considerably affected its catalytic activity. For example, even at a reaction temperature of 400 °C for the SZR, the o-xylene, toluene, and benzene conversions were 19.2, 6.3, and 12.3%, respectively. However, T_{50} and T_{90} (temperatures when the reactant conversion approached 50 and 90%, respectively) of o-xylene, toluene, and benzene conversions for the 0.1 wt% Pt/SZR catalyst were ((327 and 344), (321 and 336), and (302 and 319)) °C, respectively. An increase in the amount of platinum added to the SZR led to an increase in the conversion of each reactant. In the case of the 1.0 wt% Pt/SZR catalyst, with T_{50} and T_{90} of (302 and 319) °C, the conversions were ((282 and 296), (265 and 277), and (278 and 295)) °C, respectively. As the platinum added to the SZR increased from 0.1 to 1.0 wt%, the BET surface area increased. However, there was no significant change in the textural properties of the SZR due to the addition of platinum. The SEM images demonstrated that increasing the amount of platinum added promoted the formation of small particles on the catalyst surface. Therefore, the increase in catalytic activity by platinum addition to the SZR seemed to be attributed to the platinum species having excellent activity in oxidizing hydrocarbons. From the TPR results, an increase in the amount of platinum facilitated the lattice oxygen mobility of the catalyst, and consequently increased the catalytic activity. The TEM data indicated that the platinum particle size increased with increasing the amount of platinum added, resulting in increased active sites and increased catalytic activity. As a result, although easily moving lattice oxygen affected the increase in catalytic activity, it seemed that the increase in the active sites, such as Pt^{+2} and Pt^{+4}, had greater effect on the increase in catalytic activity.

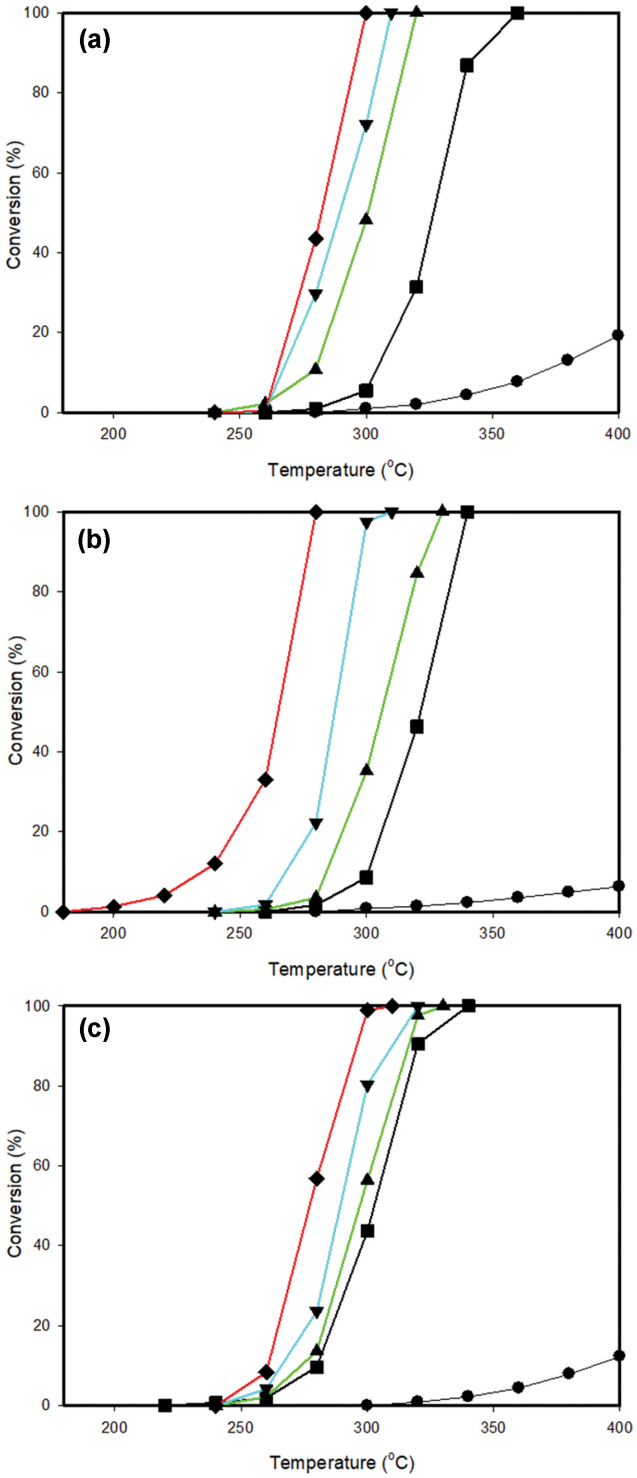

Fig. 8. o-Xylene (a), toluene (b), and benzene (c) conversions according to reaction temperature (Reaction conditions: reactant concentration=1,000 ppm, GHSV=50,000 h^{-1}). ● SZR, ■ 0.1Pt/SZR catalyst, ▲ 0.3Pt/SZR, ▼ 0.5Pt/SZR, ◆ 1.0Pt/SZR catalyst.

CONCLUSIONS

Pt/SZR was prepared to test whether zinc rods of spent batteries can serve as a catalyst material (support) for the complete oxi-

dation of VOCs. When (0.1-1.0) wt% platinum was added to the SZR, the catalytic activity increased proportionally. From the TPR results, it was found that the increase in the amount of platinum added resulted in improving the lattice oxygen mobility of the SZR. The movable lattice oxygen contributed to the enhancement of catalytic activity. The TEM results indicated that an increase in the amount of platinum added resulted in an increase in the platinum particle size, followed by an increase in active sites, thereby increasing the catalytic activity. In addition, although easily moving lattice oxygen affected the increase in catalytic activity, the increase in the active sites, such as Pt^{+2} and Pt^{+4}, had greater effect on the enhancement of catalytic activity. For the 1.0Pt/SZR catalyst, the reaction temperatures for complete oxidation of o-xylene, toluene, and benzene were 300, 280, and 310 °C, respectively, at gas hourly space velocity (GHSV) of 50,000 h^{-1}. As a result, the zinc rod of spent batteries can be used as a catalyst material (support) for VOCs oxidation.

ACKNOWLEDGEMENTS

This research was supported by the Basic Science Research Program of the National Research Foundation of Korea (NRF) funded by the Ministry of Science and ICT (2022R1A2C100639111).

SUPPORTING INFORMATION

Additional information as noted in the text. This information is available via the Internet at http://www.springer.com/chemistry/journal/11814.

REFERENCES

1. T. Dutta, K. H. Kim, A. Deep, J. E. Szulejko, K. Vellingiri, S. Kumar, E. E. Kwon and S. T. Yun, *Renew. Sustain. Energy. Rev.*, **18**(82), 3694 (2018).
2. J. Han, D. Han, M. Cui, M. Yang and L. Pan, *J. Hazard. Mater.*, **B133**, 257 (2006).
3. S. Kierkegaard, *Comput. Law Security Rep.*, **23**, 357 (2007).
4. B. J. Chen and M. Luo, *Environ. Res.*, **142**, 96 (2015).
5. W. Q. Wang, H. H. Chen, W. J. Zhao, K. M. Fang, H. J. Sun and F. Y. Zhu, *Chemosphere*, **287**, 132120 (2022).
6. C. C. B. M. De Souza, D. C. Oliveira and J. A. S. Tenorio, *J. Power Sources*, **103**, 120 (2001).
7. A. L. Salgado, A. M. O. Veloso, D. D. Pereira, G. S. Gontijo, A. Salum and M. B. Mansur, *J. Power Sources*, **115**, 367 (2003).
8. L. J. Xin and M. X. Ling, *Cryogenics*, **107**, 103060 (2020).
9. X. Shen, X. Du, D. Yang, J. Ran, Z. Yang and Y. Chen, *J. Environ. Chem. Eng.*, **9**, 106729 (2021).
10. C. Zhang, X. Gao, J. Qin, Q. Guo, H. Zhou and W. Jin, *J. Hazard. Mater.*, **402**, 123817 (2021).
11. N. T. T. Truc, T. D. Pham, D. V. Thuan, L. T. Son, D. T. Tran, M. V. Nguyen, V. N. Nguyen, N. M. Dang and H. T. Trang, *J. Alloys Compd.*, **798**, 12 (2019).
12. X. Tang, F. Feng, L. Ye, X. Zhang, Y. Huang, Z. Liu and K. Yan, *Catal. Today*, **211**, 39 (2013).
13. P. Saingam, Z. Baig, Y. Xu and J. Xi, *J. Environ. Sci.*, **69**, 133 (2018).
14. M. Tomatis, M. T. Moreira, H. Xu, W. Deng, J. He and A. M. Parvez, *J. Clean. Produc.*, **233**, 808 (2019).
15. X. Xie, J. Cao, Y. Xiang, R. Xie, Z. Suo, Z. Ao, X. Yang and H. Huang, *Appl. Catal. B: Environ.*, **309**, 121235 (2022).
16. J. J. Spivey, *Ind. Eng. Chem. Res.*, **26**, 2165 (1987).
17. D. R. Vaar, M. W. Vatavuk and A. H. Wehe, *J. Air Waste Manage. Assoc.*, **41**(4), 497 (1991).
18. W. Gao, X. Tang, H. Yi, S. Jiang, Q. Yu, X. Xie and R. Zhuang, *J. Environ. Sci.*, **125**, 112 (2023).
19. E. M. Cordi and J. L. Falconer, *J. Catal.*, **162**(1), 104 (1996).
20. P. Dégé, L. Pinard, P. Magnoux and M. Guisnet, *Surf. Chem. Catal.*, **4**(1), 41 (2001).
21. S. C. Kim, *J. Hazard. Mater.*, **B91**(1-3), 285 (2002).
22. C. H. Wang, S. S. Lin, C. L. Chen and H. S. Weng, *Chemosphere*, **64**(3), 503 (2006).
23. K. Hassan, R. Hossain, R. Farzana and V. Sahajwalla, *Anal. Chim. Acta*, **1165**, 338563 (2021).
24. M. V. Gallegos, M. A. Peluso, E. Finocchio, H. J. Thomas, G. Busca and J. E. Sambeth, *Chem. Eng. J.*, **313**, 1099 (2017).
25. Z. Zhao, B. Shen, Z. Hu, J. Zhang, C. He, Y. Yao, S.-Q. Guo and F. Dong, *J. Hazard. Mater.*, **400**, 123236 (2020).
26. Z. Zhao, H. Du, B. Shen, P. Gao, C. Huang and S.-Q. Guo, *Environ. Res.*, **212**, 113300 (2022).
27. H. Wu, L. Wang, J. Zhang, Z. Shen and J. Zhao, *Catal. Commun.*, **12**(10), 859 (2011).
28. Y. K. Park, H. Song, M. K. Kim, S. C. Jung, H. Y. Jung and S. C. Kim, *J. Hazard. Mater.*, **403**, 123929 (2021).
29. S. C. Kim, S. W. Nahm and Y. K. Park, *J. Hazard. Mater.*, **300**, 104 (2015).
30. J. Sun, T. Li, X. Li, J. Pan, X. Hao and T. Zhu, *J. Alloys Compd.*, **831**, 154871 (2020).
31. F. M. John, F. S. William, E. S. Peter and D. B. Kenneth, Handbook of X-Ray Photoelectron Spectroscopy, Phys. Electron. Inc. Minnesota (1992).
32. S. Scirè, S. Minicò, C. Crisafulli and S. Galvagno, *Catal. Commun.*, **2**(6-7), 229 (2001).
33. J. Trawczyński, B. Bielak and W. Miśta, *Appl. Catal. B Environ.*, **55**, 277 (2005).

Supporting Information

Catalytic removal of VOCs using Pt loaded on used battery derived Zn

Young-Kwon Park*, Sang-Chul Jung, Ho-Young Jung***, and Sang Chai Kim****,†**

*School of Environmental Engineering, University of Seoul, Seoul 02504, Korea
**Department of Environmental Engineering, Sunchon National University, Sunchon 57975, Korea
***Department of Environment and Energy Engineering, Chonnam National University, Gwangju 61186, Korea
****Department of Environmental Education, Mokpo National University, Muan 58554, Korea
(*Received 13 July 2022 • Revised 22 August 2022 • Accepted 4 September 2022*)

1. Section S1

Zinc rod (ZR) found in the center of spent primary batteries of R company was treated with 0.1N sulfuric acid solution to prepare the SZR. We carried out the acid treatment of ZR according to the method reported by us previously to prepare the SZR catalyst [29]. The Pt/SZR catalysts were prepared from SZR and hexachloroplatinum (H_2PtCl_6), where we adopted a conventional impregnation method to add hexachloroplatinum. In order to adjust the amount of platinum supported on the SZR catalyst, we dissolved the weighed hexachloroplatinum in 50 mL of deionized water, and added the weighed SZR catalyst to it. We stirred SZR and aqueous hexachloroplatinum mixture at 80 °C until it became a paste, and then dried at 100 °C for 20 h, before stabilizing it under air atmosphere for 4 h at 400 °C. The prepared catalyst was named as xPt/SZR, where x represents the weight percentage of platinum.

2. Section S2

The BET (Brunauer Emmett Teller) surface areas of catalysts were measured through N_2 adsorption at 77 K using a Belsorp Mini II 2020 analyser. Before sorption analysis, all catalysts were degassed in vacuum (5×10^{-3} mmHg) at 150 °C for 6 h. XRD (X-ray diffraction: a Phillips PW3123 diffractometer) was used to study the crystalline structures of the catalysts using Cu Kα radiation of 0.154 nm. Catalysts were examined in the 2θ range of 20°-90° at a scanning speed of 70° h^{-1}. H_2-TPR (hydrogen temperature programmed reduction: a BEL-CAT setup) was performed. Prior to analysis, 0.4 g of catalyst was pretreated with 30 cm^3 min^{-1} of Ar gas at 200 °C for 2 h. The temperature of the catalyst was lowered to 50 °C. A mixture of 5% H_2 gas and 95% Ar gas was used to reduce the catalyst sample. The flow rate was 30 mL min^{-1}, and the temperature was raised to 1,000 °C at a heating rate of 10 °C min^{-1}. A TECNAI F20 (Phillips, Holland) was used to obtain field emission transmission electron microscopy (FE/TEM) images at an acceleration voltage of 200 kV. The scanning electron microscopy (SEM) measurements were conducted using a SEM (JEOL JSM-6390). A HITACHI S-4800 SEM with an Oxford Link SATW ultrathin window EDX detector was used for SEM/EDX (scanning electron microscope/energy dispersive X-ray) analysis. The chemical components of the particle were determined from EDX data acquired in point mode at several spots within each particle. X-ray photoelectron spectroscopy (XPS) (VG Scientific MultiLab 2000) was performed using non-monochromatic Mg Kα radiation with an energy of 1,253.6 eV. The C1s peak (285.0 eV) obtained from XPS was used to calibrate the binding energy.

3. Section S3

A sample of the catalyst (60 mg) was placed in the middle of the reactor and supported by quartz wool. Toluene was purchased from Fisher. Air stream was passed through each toluene saturator. Each reactant concentration was 1,000 ppm, which was adjusted temperature of a saturator and by mixing with another air stream. Reactant flow was indicated by a GHSV of 50,000 h^{-1}. All lines were kept at 120 °C to prevent condensation and adsorption of the reactant and product. Inlet and outlet concentrations were measured using a GC (gas chromatograph: GC-14A, Shimadzu) equipped with a thermal conductivity detector. The column packing used for analysis consisted of 5% bentone-34 and 5% DNP/Shimalite (3 mm ø×3 m, 60-80 mesh) for benzene, toluene, and o-xylene separations, while a porapak Q (3 mm ø×3 m, 50-80 mesh) was used for CO_2 analyses. No other products were observed except CO_2 and H_2O in the reaction experiment. The conversion was calculated based on the consumption of each reactant.